

Evaluation of Potential Occupational Exposure and Release of Nanoparticles in Semiconductor-Manufacturing Environments

Zhaobo Zhang ¹, Paul Westerhoff ² and Pierre Herckes ^{1,*}

¹ School of Molecular Sciences, Arizona State University, Tempe, AZ 85297-1604, USA; zzhan223@asu.edu

² NSF Nanosystems Engineering Research Center for Nanotechnology-Enabled Water Treatment, School of Sustainable Engineering and the Built Environment, Ira A. Fulton Schools of Engineering, Arizona State University, Tempe, AZ 85287-3005, USA; p.westerhoff@asu.edu

* Correspondence: pierre.herckes@asu.edu; Tel.: +1-480-965-4497

Abstract: Occupational exposure to airborne nanoparticles in semiconductor-manufacturing facilities is of growing concern. Currently, comprehensive information regarding atmospheric concentrations, potential origins, and the physical and chemical properties of nanoparticles in these industrial settings is lacking. This study investigated the occurrence of airborne nanoparticles within a semiconductor-research and -manufacturing facility, during both routine operation and maintenance activities. A Scanning Mobility Particle Sizer was used to monitor size-resolved airborne-nanoparticle number concentrations spanning the range of 6 to 220 nm. Breathing zone filter samples were also collected during maintenance processes and underwent subsequent analyses via Transmission Electron Microscopy and Inductively Coupled Plasma Mass Spectrometry, to discover the size, morphology, and chemical composition of the observed nanoparticles. The findings reveal low levels of airborne nanoparticles during routine operations, but maintenance tasks resulted in substantial concentration surges particularly for plasma-enhanced chemical vapor deposition tools with concentrations up to 11,800 particles/cm³. More than 80% of observed particles were smaller than 30 nm. These smallest particles were predominately composed of metals such as iron, nickel, and copper. Moreover, larger particles above 100 nm were also identified, comprising process-related materials such as silicon and indium. Comparative assessment against established mass-based exposure limits did not yield any exceedances. Current exposure limits do not typically consider size though, and the preponderance of small nanoparticles (<30 nm) would warrant a more size-differentiated exposure-risk assessment.

Keywords: semiconductor-manufacturing environment; nanoparticle exposure; personal sampling; scanning mobility particle sizer; particle size distribution

Citation: Zhang, Z.; Westerhoff, P.; Herckes, P. Evaluation of Potential Occupational Exposure and Release of Nanoparticles in Semiconductor-Manufacturing Environments. *Atmosphere* **2024**, *15*, 301. <https://doi.org/10.3390/atmos15030301>

Academic Editors: Chien-Cheng Jung and Wei Hsiang Chang

Received: 29 January 2024

Revised: 20 February 2024

Accepted: 22 February 2024

Published: 28 February 2024



Copyright: © 2024 by the authors. Licensee MDPI, Basel, Switzerland. This article is an open access article distributed under the terms and conditions of the Creative Commons Attribution (CC BY) license (<https://creativecommons.org/licenses/by/4.0/>).

1. Introduction

Industrial cleanrooms are specialized environments, designed to maintain high levels of cleanliness based on particle number concentrations, resolved using size, as classified by the International Standardization Organization (ISO) [1]. In the semiconductor industry, high-level cleanrooms typically utilize laminar airflow combined with High-Efficiency Particulate Air filters (HEPA) to minimize airborne particles [2]. This approach is used in both fabrication and sub-fabrication areas, with the goal of preventing potential defect formation in the final product. However, with the growing use of engineered nanomaterials (ENM) in production processes, such as in chemical mechanical planarization (CMP) slurries [3–5], there is an emerging concern that ENMs may become aerosolized, leading to potential occupational exposure [6], and release into the environment, especially during maintenance operations [7].

Observational studies on aerosol concentration and composition are scarce in the scientific literature, as these environments tend to be, by definition, clean so present low

concentrations, and only a few studies exist, especially on nanoparticles [8,9]. Shepard and Brenner observed a 7.6-fold increase in airborne nanoparticles, ranging from 11.5 to 115.5 nm in size, during a CMP tool set-up process [10]. Subsequently, Brenner et al. conducted further assessments during CMP maintenance processes and reported a spike in airborne nanoparticle occurrence ($\sim 18,000$ #/cm³), while workers vacuumed the dried slurry [8]. Most of the particles in CMP areas were characterized at a size over 100 nm and composed of silicon, aluminum, and cerium (suggesting material from the CMP slurry) [8,11,12]. Other manufacturing processes like diffusion, wet etching, chemical vapor deposition (CVD), metallization, ion implantation, and dry etching have also been investigated by previous studies [9,13,14]. Maintenance processes were identified as the main contributors to airborne particle release and exposure. Liao et al. reported spikes of 921,500 #/cm³ and 647,000 #/cm³ in airborne particle concentration during ion implanter and plasma enhanced chemical vapor deposition (PECVD) tool-maintenance processes, respectively, with all particles nanosized (<60 nm) [9]. This also suggests the formation and release of incidental, process-generated nanoparticles and raises significant concern in terms of release and worker exposure during maintenance. However, due to the lack of characterization information, it is hard to evaluate the potential exposure risks.

Airborne-particle exposure in the semiconductor industry has been associated with reproductive risks, non-Hodgkin's lymphoma, leukemia, brain tumors, and breast cancer [15,16]. The release of III-V material particles, including indium arsenide (InAs), gallium arsenide (GaAs), and Indium Tin Oxide (ITO) during semiconductor-manufacturing processes could induce cytotoxicity, impact the respiratory system, and damage the liver or kidney [17–19]. The National Institute for Occupational Safety and Health (NIOSH) has established recommended exposure limits (RELs), while the Occupational Safety and Health Administration (OSHA) has set permissible exposure limits (PELs) for occupational exposure. The American Conference of Governmental Industrial Hygienists (ACGIH) has set threshold limit values (TLVs). In nearly all cases, the regulations are mass-based and do not differentiate between sizes of airborne particles or consider the unique toxicity considerations for nanoparticles due to their small size, high surface area, and unique physicochemical properties [20,21]. To date, only ultrafine titanium dioxide and carbon nanotubes have a size-resolved exposure limit [22,23]. However, increasing evidence that highlights the risks associated with nano-sized particle exposure, which may more easily cross biological barriers and translocate in the human body [24–27], raises concern. Finally, it is noteworthy that while the international organization for standardization (ISO) has established cleanroom classifications that are based on size-resolved-particle number concentration, as outlined in ISO 14644-1 [1], nanoparticles (smaller than 100 nm) are not currently considered.

This study aims to quantify the occurrence of nanoparticles in semiconductor-type cleanroom facilities through in situ online observation and filter-based offline characterization methods. We measure the release and resulting exposure to airborne nanoparticles in various semiconductor-manufacturing processes, during routine and preventive maintenance operations. This study provides detailed characterization results, including particle number size distribution, morphology, chemical composition, and elemental mass concentration. By enhancing the characterization of airborne nanoparticles in semiconductor facilities, this study hopes to inform the management of occupational exposure risks associated with airborne nanoparticles.

2. Materials and Methods

2.1. Sampling Site

Sampling was conducted at two locations: the ASU Nanofab facility (Figure 1a, <https://cores.research.asu.edu/nanofab> [accessed on 9 May 2023]) and Macro Technology Works (MTW, Figure 1b, <https://engineering.asu.edu/macrotechnology-works> [accessed on 9 May 2023]). The Nanofab has an ISO level 5 cleanroom (Class 100), and sampling

focused on the PECVD tool and the wet etching areas. MTW, a research facility affiliated with ASU, has a pilot-scale cleanroom equipped with a suspended floor, laminar airflow system, and sub-fab loading area. The air system features a fab area and a return air area, both conforming to ISO level 5. The fab area uses a HEPA filter and controls laminar flow from the ceiling to the ground, while the return air area receives the fab area air in a ground to ceiling laminar flow. Sampling was conducted near tools in the return air area (PECVD, fluorine etching, chlorine etching, and dry etching) and in the fab area (plasma etching, sputtering, and plasma asher).

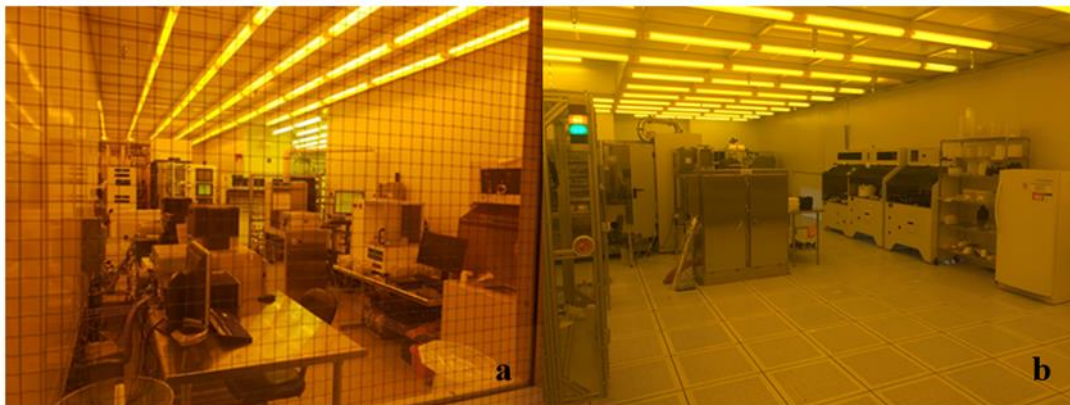


Figure 1. Sampling location at ASU (a) Nanofab and (b) MTW cleanrooms.

2.2. Field Observations

In this study, the size-resolved airborne nanoparticle number concentration, ranging from 6 to 220 nm, was monitored using a Scanning Mobility Particle Sizer (SMPS). The SMPS consisted of a differential mobility analyzer (DMA, TSI 3081, TSI Inc., Shoreview, MN, USA) and a condensational particle counter (CPC, TSI 3752, TSI Inc., Shoreview, MN, USA), providing number counts resolved in 91 size bins in real time within 70 s, with an accuracy within 5% in both size and concentration measurements [28,29]. The inlet flow rate and sheath flow were set at 1.5 L/min and 15 L/min, respectively. The SMPS was positioned on a cart approximately 1 m above the ground, in close proximity (within 1 m) to the targeted tools (Figure 2). Sampling activity commenced at the beginning of preventive maintenance operation and continued until midnight after the operation, aiming at monitoring changes in airborne nanoparticle concentrations during and after maintenance activities. The timing of maintenance activities was recorded to correlate with changes in airborne nanoparticle concentrations to identify specific operations that lead to high particle concentrations.



Figure 2. SMPS configuration employed for field observation at the (a) PECVD (I), (b) Fluorine etching, (c) sputtering (I), and (d) plasma etching areas in the MTW cleanroom.

2.3. Filter-Based Sample Collection

Aerosol samples were collected using 25 mm, 0.8 μm pore sized mixed cellulose ester (MCE) filters (#225-19, SKC Inc., Eighty Four, PA, USA), recommended by NIOSH for chemical hygiene protocols (conforming to NIOSH 7300 and NIOSH 7402) [30,31]. The filters were placed in 25 mm plastic filter cassettes (#225-2-25LF, SKC Inc., Eighty Four, PA, USA) and attached to the worker's collar using a filter holder (#225-1, SKC Inc., Eighty Four, PA, USA) to collect breathing-zone samples. Samples were collected using personal samplers at a flow rate of 5 L/min (Leland legacy pump, SKC Inc., Eighty Four, PA, USA).

Previous study [11] reported challenges for working in clean room environments because of low ambient concentrations and relatively high filter blanks. To minimize blanks values, MCE filters were subjected to soaking in 0.6 M hydrochloric acid (Trace metal grade, Sigma Aldrich, St. Louis, MO, USA) overnight, followed by thorough rinsing with ultra-pure water ($>18.2 \text{ M}\Omega\text{-cm}$) prior to sampling work [32]. All filter samples were promptly stored in a refrigerator at 4 $^{\circ}\text{C}$ upon completion until further analysis.

2.4. ICP-MS Analysis

Filter samples were analyzed for the elemental mass concentration using Inductively Coupled Plasma–Mass Spectrometry (ICP-MS, NexION 2000, Perkin Elmer Inc., Waltham, MA, USA) after acid-assisted microwave digestion. In brief, prior to digestion, each container used in this protocol (Teflon vessel, Teflon beaker, plastic volumetric flask) was pre-cleaned with a 10% HNO_3 soak overnight. Filter samples were digested in a 20

mL Teflon vessel (Xpress, CEM Corporation, Matthews, NC, USA) via microwave (Mars 5, CEM Corporation, Matthews, NC, USA) using a solution of 10 mL HNO₃ + 4 mL H₂O + 1 mL HF. Trace metal grade acids (HNO₃, HF; Sigma Aldrich, St. Louis, MO, USA) and ultra-pure water (>18.2 MΩ·cm) were used in the protocol to minimize the reagent background. Detailed information on microwave settings is provided in Table S1 [33]. Following microwave digestion, the vessel contents were evaporated at 160 °C in a 75 mL Teflon beaker until 1 mL of solution remained to remove HF, which could potentially damage the instrument. The residual was then diluted with 2% HNO₃ to 50 mL for a subsequent ICP-MS analysis. All sample preparation was conducted in the cleanrooms of the Metals, Environmental, and Terrestrial Analytical Laboratory at ASU.

2.5. STEM Analysis

The morphology of the collected particles was investigated using a Scanning Transmission Electron Microscope (STEM, ARM200F, JEOL Inc., Pleasanton, CA, USA). An Energy Dispersive X-ray Spectroscopy (EDX, Ultim Max, Oxford Instruments, Abingdon, UK) was employed to determine the elemental composition of selected particles. To prepare the samples for the analysis, a filter section was sonicated in 20 mL of 200 proof ethanol (Sigma Aldrich, St. Louis, MO, USA). The suspension was then evaporated under a fume hood without heating to concentrate the solution. The suspension was then transferred onto a 200-mesh copper grid (Ted Pella Inc., Redding, CA, USA) using an acid-cleaned micropipette tip. The grid with the suspended particles was directly loaded into the instrument for analysis. Randomly selected particles on the grid were imaged, and EDX elemental mapping was performed.

3. Results and Discussion

3.1. Particle Number Concentration

Table 1 summarizes the observations on airborne particle number concentration during preventive maintenance activities, normal operational processes, and nocturnal background measurements. Particle number concentrations are reported in units of particles per cubic centimeter (#/cm³), as measured by SMPS using the electrical mobility diameter within the range of 6–220 nm.

Table 1. Summary of particle counts (6–220 nm) recorded in different areas during routine operation.

Sampling Equipment	Sampling Area	Nocturnal Background ^c (#/cm ³) ^d	Working Hour ^e (#/cm ³)	Maintenance Activity (#/cm ³)	Maintenance Duration (min)	Maximum Value (#/cm ³)
PECVD I ^a	MTW return air	21	15	321	21	4120
PECVD II	Nanofab	7	313	476	90	11,800
Plasma etching	MTW fab	2	2	7	30	90
Dry etching	MTW return air	89	139	260	20	1380
Fluorine etching	MTW return air	54	16	523	12	1470
Chlorine etching	MTW return air	2	14	4	26	40
Wet etching ^b	Nanofab	15	201	N/A	N/A	N/A

Sputtering I	MTW fab	8	10	718	32	3440
Sputtering II	MTW fab	12	15	215	60	1380
Plasma Asher	MTW fab	14	23	16	30	54

Note a: Two different instruments are distinguished with I and II. Note b: The wet etching acid hood has no observable maintenance activity. Note c: The nocturnal period corresponds to the mean particle number concentration recorded between 21:00 and 24:00 on a normal operation day, during which no operational work was carried out. Note d: The concentration is reported as particle counts per cubic centimeter, using the SMPS default measurement range of 6–220 nm. Note e: The working hour period refers to the average particle number concentration recorded between 9:00 and 12:00 on a normal operation day. N/A: Not applicable.

The airborne nanoparticle concentration during routine operation were presented as 3 h average values measured on a normal operation day, specifically over 9:00–12:00 and 21:00–24:00, respectively. Table 1 shows that the nocturnal background particle concentrations vary among different sampling locations. The ASU Nanofab area showed concentrations ranging from 7 to 15 #/cm³, while the MTW fab area recorded consistent concentration ranging from 2 to 14 #/cm³. The MTW return air areas exhibited higher particle concentrations, ranging from 2 to 89 #/cm³.

On a routine operation day, the ASU Nanofab exhibited a significant increase in particle number concentrations for both PECVD and wet etching areas. The concentrations rose from 7 #/cm³ and 15 #/cm³ to 313 #/cm³ and 201 #/cm³, respectively, during working hours. This increase is associated with heightened occupancy during these hours due to research and training activities. In contrast, MTW did not exhibit this trend, reflecting lower occupancy levels as it operates continuously with a limited operator presence in the cleanroom. However, these conditions change during maintenance operations. In the present study, sampling was performed during preventive maintenance activities, specifically when technicians vent and access the vacuum chambers to clean the chamber surfaces using humidified fabrics before resealing and reestablishing a vacuum. The entire process typically lasts for 30 min, unless unexpected issues arise (Table 1).

Preventive maintenance significantly affected the occurrence of particles in the environment of some tools. Both PECVD tool areas in Nanofab and in MTW experienced significant airborne-particle increases (618 #/cm³ and 375 #/cm³ from 313 #/cm³ and 22 #/cm³, respectively). During the MTW PECVD tool-maintenance processes, a spike in particle counts of up to 4120 #/cm³ was detected, two orders of magnitude higher than during routine operation. This is consistent with a previous report by Liao et al. who observed an even higher spike (647,000 #/cm³) during PECVD tool maintenance [9].

Etching tools exhibited different results, based on the specific instruments sampled. Notably during chlorine etching and dry-etching-tool-maintenance processes, airborne nanoparticle concentrations increased with concentrations rising from 16 #/cm³ and 139 #/cm³ to 523 #/cm³ and 260 #/cm³, respectively, consistent with previous reports by Choi et al. [13], indicating that maintenance processes can elevate particle concentrations 2–4 times higher than during normal operation processes for dry-etching tools. In contrast, no significant increase in particle number concentration was observed during maintenance processes for fluorine and plasma etching.

Our observational study is the first one to also investigate sputtering tools and plasma asher environments during maintenance procedures. Both sputtering tool areas tested exhibited increased airborne particle concentrations during maintenance (from 10 #/cm³ and 15 #/cm³ to 718 #/cm³ and 227 #/cm³), while concentrations in the vicinity of the plasma asher remained consistently low (from 2 #/cm³ to 7 #/cm³).

3.2. Particle Concentration Temporal Change during Maintenance

Figure 3 displays the evolution over time of particle concentrations during maintenance processes for the PECVD (II) and sputtering tools (I) located in MTW. The heat map highlights the two specific events with the highest maximum spike (Figure 3a) and highest maintenance average (Figure 3b) in terms of particle number concentration, the color dots on the heat map indicate the size-resolved-particle number concentration at specific moment. The light-purple background means no particles have been detected during the monitoring processes.

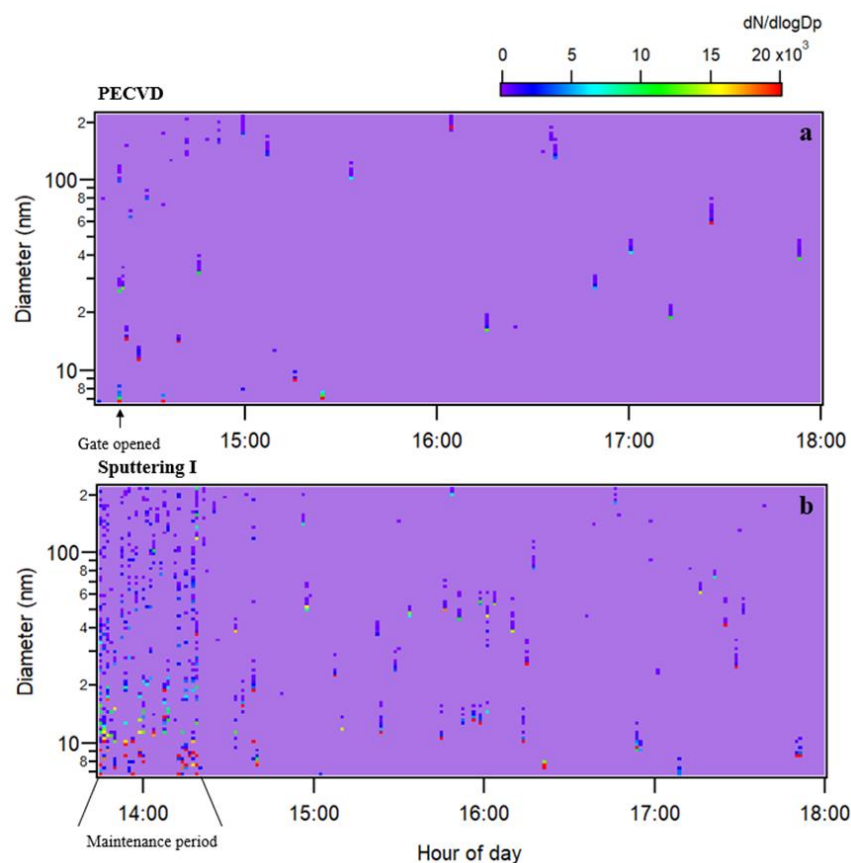


Figure 3. Heat maps for observation results collected in MTW from start of maintenance until same day 18:00 for (a) PECVD tool (II) and (b) sputtering tool (I). The color scale represents the particle number concentration expressed as $dN/d\log D_p$, with a measurement range of 6–220 nm.

In Figure 3a the maintenance day on the PECVD tool is shown. The SMPS recording started at 14:13, and the PECVD vacuum chamber was opened at 14:20. A spike in particle concentration (4120 \#/cm^3) was detected using the SMPS at the same time as the chamber gate was opened, suggesting the release of particles from inside the vacuum chamber or potentially the generation of new particles upon contact with ambient air [14]. The strong laminar air flow within the cleanroom effectively removed the particles, resulting in a rapid decrease (4120 \#/cm^3 to 225 \#/cm^3 in next SMPS scan). Overall, throughout the entire PECVD tool-maintenance processes only a few particle spikes were recorded resulting in an average particle number concentration of 321 \#/cm^3 , which is significantly higher than the background concentration during routine operation (15 \#/cm^3).

Figure 3b shows the particle concentration observations during sputtering-tool (I) maintenance, which presented the highest average concentration of airborne particles (718 \#/cm^3) and a peak value of 3440 \#/cm^3 . In contrast to the observations for the PECVD (II) tool, the airborne nanoparticle concentration during sputtering (I)-tool maintenance remained consistently high throughout the entire period with less-significant peaks. After

maintenance, the airborne nanoparticle levels rapidly decreased to ~ 166 $\#/cm^3$ and eventually back to the background level (8 $\#/cm^3$) at nighttime. The sputtering tool exhibited a higher number of particles, measuring over 100 nm compared to the PECVD tools; additional discussion is provided in the next section. For reference, heat maps for all tool-maintenance activities are available in Figure S1.

3.3. Particle Size Distribution for Airborne Particles

Based on the heat maps in Figures 3 and S1, most particles detected during maintenance events were smaller than 30 nm. To highlight the abundance of small nanoparticles, the total airborne nanoparticle counts were categorized into three size ranges (6 – 30 nm, 30 – 100 nm, and 100 – 220 nm) and summarized in Figure 4.

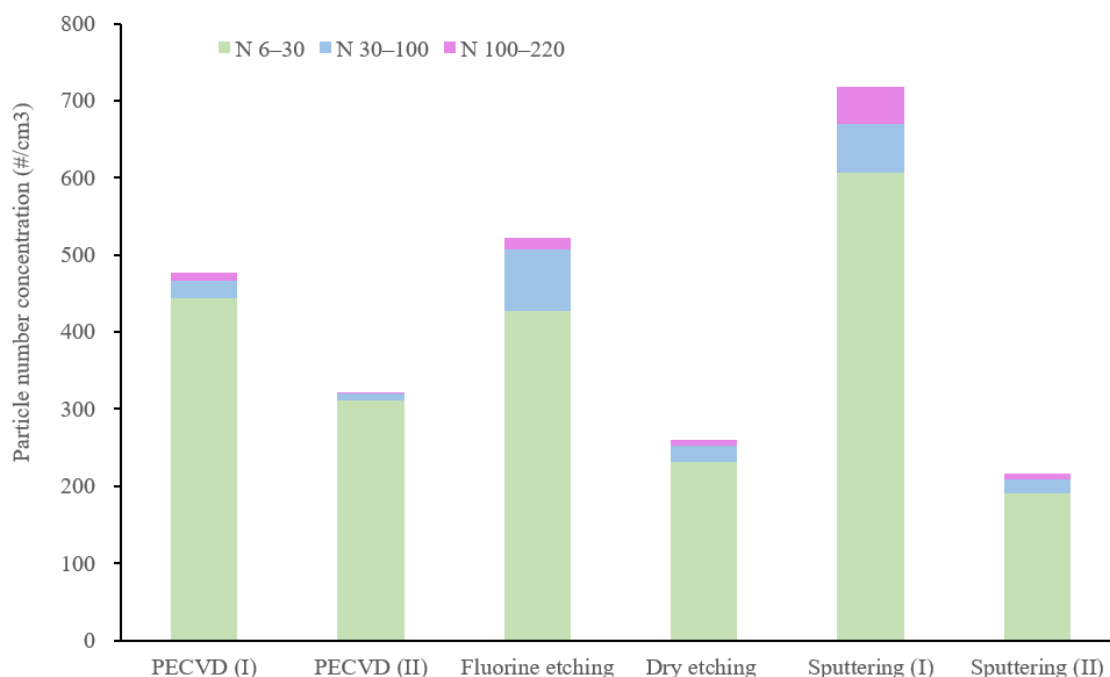


Figure 4. The average particle number concentrations in the size ranges of 6 – 30 nm, 30 – 100 nm, and 100 – 220 nm during maintenance operations. Only tools that exhibited significant particle increase during maintenance processes are listed.

In Figure 4, smaller sized nanoparticles (N_{6-30}) dominate the observed particles during maintenance, comprising over 80% of particles for each sampled tool. This aligns with previous studies reported by Liao et al. [9], where the particles in the size range of 9 – 20 nm was the dominant species released during PECVD tool-maintenance processes. The overall number of nanoparticles observed during maintenance activities did not seem to influence the size distribution. For example, despite the highest average count of sputtering (I) (718 $\#/cm^3$) compared to the sputtering tool (II) (260 $\#/cm^3$), the relative importance of the N_{6-30} fraction was similar for both tools at 84% and 88% , respectively. Overall, the PECVD tools, in our study, released more N_{6-30} (93% , 97%) compared to etching (82% , 89%) and sputtering tools (84% , 88%), which have relatively higher number concentrations of larger particles (N_{30-100} and $N_{100-220}$). This finding may be attributed to differences in particle formation mechanisms for each type of manufacturing tool. In the next section, we will investigate this further by looking at the morphology and chemistry of the particles.

3.4. Morphology and Elemental Composition of Collected Airborne Particles within Breathing-Zone Filter Sample

Based on the particle size distribution depicted in Figure 4, the majority of particles observed during maintenance processes were smaller than 30 nm. STEM analysis of breathing-zone filter samples, as shown in Figure 5a, confirmed the presence of these small particles; a metallic copper nanoparticle (Oxygen signal not enhanced) with a size around 10 nm was identified in the PECVD sample. Larger particles (30–220 nm) were also observed in this PECVD sample. Figure 5b shows a 50 nm oxidized silicon particle with trace aluminum mixed in (EDX spectra available in Figure S2), which may have originated from silica nanoparticles generated during the PECVD operation process for thin film, as indicated using the reaction below.

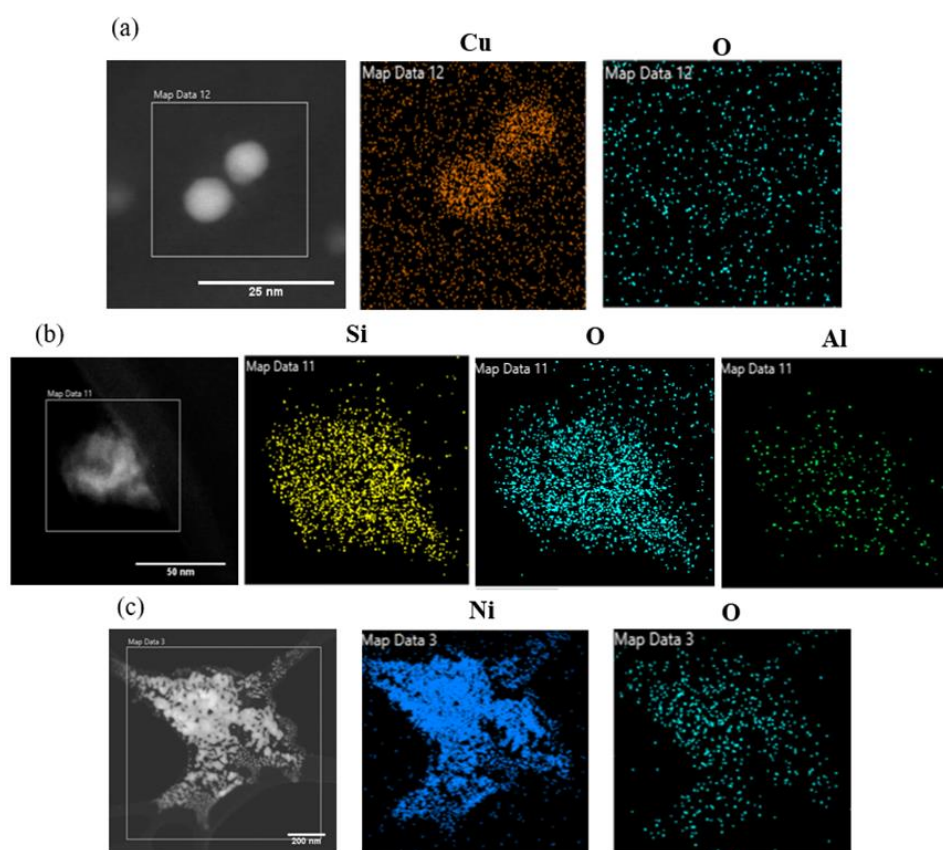
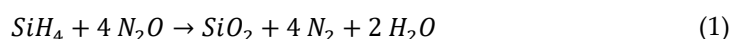


Figure 5. Selected STEM image of particles with EDX elemental mapping for airborne particulate matters collected within worker breathing-zone areas during PECVD tool-maintenance processes. (a) Tiny particles (<10 nm) composed of copper (oxygen signal not enhanced). (b) Oxidized silicon particle (~50 nm) with trace aluminum mixed in. (c) Agglomeration (>1 μm) of small metallic nickel particles (91.2 wt% Ni).

Furthermore, particles exceeding the measurement range of SMPS (>220 nm) were observed. Figure 5c illustrates a nickel particle with a size over 1 μm , presumably formed by the agglomeration of smaller nanoparticles and predominantly composed of metallic nickel (91 wt% Ni, EDX spectra available in Figure S3) [34].

To confirm the consistency of these findings, breathing-zone samples collected during the maintenance process of the sputtering tool were also analyzed. Figures S4–S6 display particles smaller than 30 nm, predominantly composed of transition metals such as copper, iron, and nickel. Additionally, Figure S7 exhibits a larger particle of approximately 100 nm in size, composed of oxidized indium. This particle is process-

related, as indium-tin-oxide was employed as the sputtering target. Larger particles exceeding 1 μm in size were also detected, but they did not exhibit agglomeration characteristics (Figure S8). These particles were primarily composed of process-related elements from the sputtering target, including indium, aluminum, titanium, and zirconium.

In our observations, smaller nanoparticles (<30 nm) predominantly consisted of transition metals. This finding is interesting, considering that transition metals, especially copper, are rarely used in semiconductor products. Further investigation is necessary to determine the sources of these nanoparticles. In contrast, larger nano-particles (>30 nm) are likely to be associated with the manufacturing processes and can be related to process activities. The occasional very large particles (>1 μm), also process related, are significantly contributing to the particle mass. Assessing exposure risk in compliance with current regulations emphasizes the mass concentration over particle number counts.

3.5. Mass Concentrations in Breathing Zone Area

The previous sections highlighted the significance of nanoparticles in terms of number concentrations. However, samples collected on filters in the devices worn near the breathing zone by workers also contained larger particles that fall outside the observation range of the SMPS. These larger particles are of concern for occupational exposure, particularly for metals like indium, as they can contribute to significant mass concentrations. To assess the potential risk, we performed bulk analysis and compared the total mass concentration of breathing-zone samples with established exposure limits set by organizations such as NIOSH, OSHA, ACGIH, and CAL/OSHA. Due to the short duration of our sampling periods, we normalized the mass concentration to an eight-hour time-weighted average (8 h-TWA), which is a standard unit in regulations and allow us to make the comparison to assess whether exposure exceeds the current limit. The equation used for the normalization is shown below, where C_m is the total air mass concentration of specific elements and t_m is the duration of maintenance activity, 480 min represents the eight-hour working time.

$$8h\ TWA = \frac{C_m * t_m}{480} \quad (2)$$

Extrapolating the exposure to an eight-hour period may not be unreasonable, considering that workers may move from one tool maintenance to another. However, it's important to note that this assumption is made. Additionally, we assume all the particles collected in this study are inhalable since most of the particles collected in this study are nanoparticles.

Figure 6 shows the 8 h-TWA mass concentration of elements in the breathing-zone samples of the operators during maintenance. Silicon and aluminum are the most abundant elements, as expected due to the processing of silicon materials in each tool and the ubiquity of aluminum as a tool component material. Aluminum is also used as a target in the sputtering (I) process which resulting in yield the highest concentration (~2 $\mu\text{g}/\text{m}^3$) and at least four times higher than others. Transition metals such as zinc, iron, nickel, copper, and chromium are consistently present in the breathing zone but at lower concentrations. It is noteworthy that these are research and pilot facilities which will change targets and use at times experimental materials, less common in routine production. Indium is only observed in the sample collected from sputtering I tool, which is consistent with the use of an indium-tin-oxide target. These results are consistent with the STEM analysis.

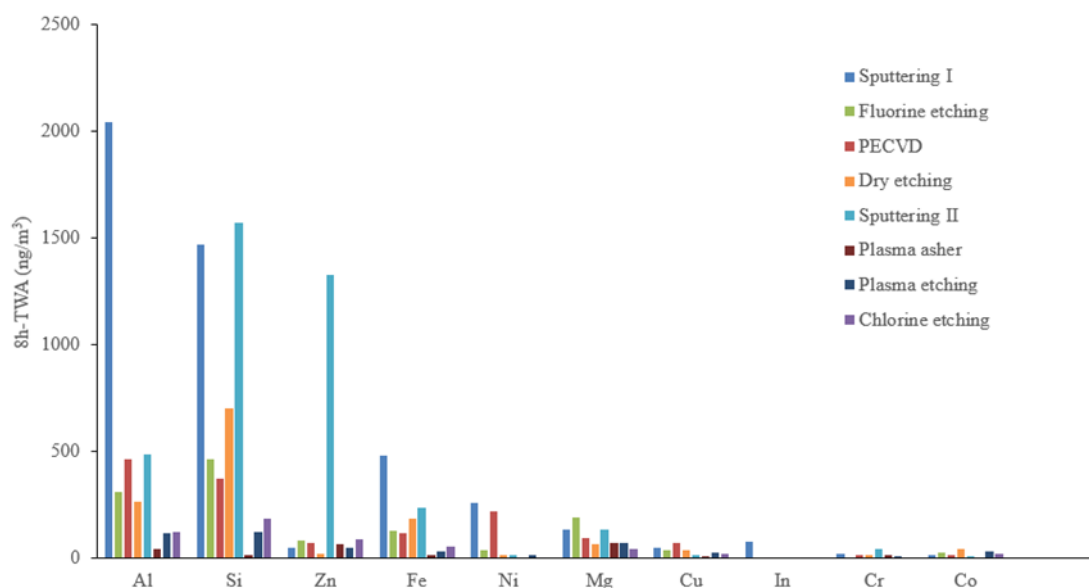


Figure 6. The mass concentration of major elements was measured in a breathing-zone sample collected during tool-maintenance processes. The concentration data were normalized to an 8 h time-weighted average (8 h TWA).

Table S2 summarizes current workplace limits for selecting elements across different regulatory agencies [35]. These limits tend to be, for most species, in the milligram or hundreds of micrograms range, whereas our results are mostly in the nanogram range (Figure 6), and hence, they are several orders of magnitude lower than the exposure limits. For example, the highest mass concentration of aluminum in the sputtering (I) sample was $\sim 2 \mu\text{g}/\text{m}^3$, which is thousands of times lower than the minimum respirable exposure level regulated by ACGIH ($1000 \mu\text{g}/\text{m}^3$). The highest measured nickel concentration in our samples was $\sim 0.3 \mu\text{g}/\text{m}^3$ from the PECVD tool, which is the closest one to a limit value ($15 \mu\text{g}/\text{m}^3$) but still 50-fold lower [35]. Although none of the compounds exceeded the exposure limits in our study, it is important to note that current limitations are primarily mass-based, while the toxicity of nanoparticles may differ from bulk material. Additionally, the airborne nanoparticle exposure may vary depending on factors such as the instrument type, working load, maintenance frequency, and engineering control applications. Conducting measurements in different fabs would contribute to a better understanding of overall airborne nanoparticle occurrence in semiconductor-manufacturing environments.

3.6. Study Limitations

This study aimed to investigate the release of nanoparticles and exposure to nanoparticles in semiconductor environments. A variety of tools were tested in two different facilities. This is, of course, a limited set of observations, but they were challenging to overcome for practical reasons. It is clear that there will likely be significant variability between facilities and between tools. The facilities and tools tested here were modern and at least pilot scale tools, but older as well as newer technologies and processes exist. This will lead to different emissions. Finally, even for the same tool, different processes and engineering control implementations could yield different particle formations and exposures, both in terms of nature and amounts. This cannot all be captured in a single study but would require a larger community effort.

4. Conclusions

This study investigated the presence of airborne nanoparticles in semiconductor-manufacturing environments. Through in situ observational studies conducted within

two ISO level 5 cleanrooms, we found that maintenance activities led to the release and occurrence of airborne nanoparticles. These nanoparticles' concentrations increase by one to two orders of magnitude during tool maintenance and typically continued until the end of the maintenance processes. Notable concentration spikes were observed in certain instances, particularly at the opening of vacuum chambers, in a sudden surge in particle number concentration by two or more orders of magnitude. In most cases, a substantial fraction, accounting for over 80% of the observed particles, had a size smaller than 30 nm.

To further characterize the observed particles, filter-based sampling (within worker's breathing zone) and subsequent instrumental analyses including STEM and ICP-MS were used. STEM imaging demonstrated that the tiniest particles (less than 30 nm) were mainly composed of transition metals such as copper, nickel, and iron, with some particles appearing in metallic form. On the other hand, larger particles (greater than 30 nm) were associated with manufacturing materials. Additionally, a few particles larger than 1 μm were also detected. The study also analyzed the mass concentration of each element present in the filter samples and compared them to the regulations set by government agencies. Encouragingly, none of the elements exceeded the regulatory levels, with concentrations at least 50-fold lower than the limits specified by the regulations.

Although the elemental mass concentration results do not exceed exposure limits, one has to consider that most released particles are less than 30 nm in size, for which we are lacking toxicity studies that address their potentially differential toxicity from larger particles. The results clearly identify a need to further investigate the potential health effects of nanosized particles. In the meantime, it might be appropriate to consider engineering controls during maintenance operations to limit the exposure of operators and the release of nanoparticles to the clean room environment.

Supplementary Materials: The following supporting information can be downloaded at <https://www.mdpi.com/article/10.3390/atmos15030301/s1>. Figure S1: Heat map of observation results collected in other sampling area; Figure S2: EDX spectrum of Figure 5b; Figure S3, EDX spectrum of Figure 5c; Figure S4: oxidized nickel nanoparticle detected within sputtering tool sampling area; Figure S5: two metallic copper nanoparticles were detected within sputtering tool sampling area; Figure S6: metallic iron nanoparticle detected within sputtering tool sampling area; Figure S7: oxidized Indium nanoparticle detected within sputtering tool sampling area; Figure S8, mixed element particle (>1 μm) detected within sputtering tool sampling area; Table S1: microwave setting for digestion process; Table S2: exposure limits of select compounds found in breathing-zone sample.

Author Contributions: Conceptualization, Z.Z., P.W. and P.H.; methodology, Z.Z., P.W. and P.H.; software, Z.Z.; formal analysis, Z.Z.; investigation, Z.Z.; data curation, Z.Z.; writing—original draft preparation, Z.Z.; writing—review and editing, Z.Z., P.W. and P.H.; visualization, Z.Z.; supervision, P.W. and P.H.; funding acquisition, P.W. and P.H.; All authors have read and agreed to the published version of the manuscript.

Funding: This work was fully funded by Semiconductor Research Corporation (2818.007).

Institutional Review Board Statement: Not applicable.

Informed Consent Statement: Not applicable.

Data Availability Statement: The data presented in this study are available on request from the corresponding author. The data are not publicly available due to confidentiality agreements with the facilities but requests can be evaluated on a case by case basis.

Conflicts of Interest: The authors declare no conflicts of interest.

References

1. *ISO 14633-1 2015; Cleanrooms and Associated Controlled Environments—Part 1: Classification of Air Cleanliness.* ISO: Geneva, Switzerland, 1999.
2. Choi, K. Airborne PM_{2.5} Characteristics in Semiconductor Manufacturing Facilities. *AIMS Environ. Sci.* **2018**, *5*, 216–228. <https://doi.org/10.3934/environsci.2018.3.216>.

3. Speed, D.; Westerhoff, P.; Sierra-Alvarez, R.; Draper, R.; Pantano, P.; Aravamudhan, S.; Chen, K.L.; Hristovski, K.; Herckes, P.; Bi, X.; et al. Physical, Chemical, and in Vitro Toxicological Characterization of Nanoparticles in Chemical Mechanical Planarization Suspensions Used in the Semiconductor Industry: Towards Environmental Health and Safety Assessments. *Environ. Sci. Nano* **2015**, *2*, 227–244. <https://doi.org/10.1039/c5en00046g>.
4. Dumitrescu, E.; Karunaratne, D.P.; Babu, S.V.; Wallace, K.N.; Andreescu, S. Interaction, Transformation and Toxicity Assessment of Particles and Additives Used in the Semiconducting Industry. *Chemosphere* **2018**, *192*, 178–185. <https://doi.org/10.1016/j.chemosphere.2017.10.138>.
5. Zazzera, L.; Mader, B.; Ellefson, M.; Eldridge, J.; Loper, S.; Zabasajja, J.; Qian, J. Comparison of Ceria Nanoparticle Concentrations in Effluent from Chemical Mechanical Polishing of Silicon Dioxide. *Environ. Sci. Technol.* **2014**, *48*, 13427–13433. <https://doi.org/10.1021/es5029124>.
6. Bocca, B.; Battistini, B.; Leso, V.; Fontana, L.; Caimi, S.; Fedele, M.; Iavicoli, I. Occupational Exposure to Metal Engineered Nanoparticles: A Human Biomonitoring Pilot Study Involving Italian Nanomaterial Workers. *Toxics* **2023**, *11*, 120. <https://doi.org/10.3390/toxics11020120>.
7. Park, D.-U.; Zoh, K.E.; Jeong, E.K.; Koh, D.-H.; Lee, K.-H.; Lee, N.; Ha, K. Assessment of Occupational Health Risks for Maintenance Work in Fabrication Facilities: Brief Review and Recommendations. *Saf. Health Work* **2023**, *in press*. <https://doi.org/10.1016/j.shaw.2023.11.010>.
8. Brenner, S.A.; Neu-Baker, N.M.; Caglayan, C.; Zurbenko, I.G. Occupational Exposure to Airborne Nanomaterials: An Assessment of Worker Exposure to Aerosolized Metal Oxide Nanoparticles in a Semiconductor Fab and Subfab. *J. Occup. Environ. Hyg.* **2016**, *13*, D138–D147. <https://doi.org/10.1080/15459624.2016.1183012>.
9. Liao, B.X.; Tseng, N.C.; Li, Z.; Liu, Y.; Chen, J.K.; Tsai, C.J. Exposure Assessment of Process By-Product Nanoparticles Released during the Preventive Maintenance of Semiconductor Fabrication Facilities. *J. Nanoparticle Res.* **2018**, *20*, 203. <https://doi.org/10.1007/s11051-018-4302-7>.
10. Shepard, M.N.; Brenner, S. An Occupational Exposure Assessment for Engineered Nanoparticles Used in Semiconductor Fabrication. *Ann. Occup. Hyg.* **2014**, *58*, 251–265. <https://doi.org/10.1093/annhyg/met064>.
11. Brenner, S.A.; Neu-Baker, N.M.; Eastlake, A.C.; Beaucham, C.C.; Geraci, C.L. NIOSH Field Studies Team Assessment: Worker Exposure to Aerosolized Metal Oxide Nanoparticles in a Semiconductor Fabrication Facility. *J. Occup. Environ. Hyg.* **2016**, *13*, 871–880. <https://doi.org/10.1080/15459624.2016.1183015>.
12. Brenner, S.A.; Neu-Baker, N.M. Occupational Exposure to Nanomaterials: Assessing the Potential for Cutaneous Exposure to Metal Oxide Nanoparticles in a Semiconductor Facility. *J. Chem. Heal. Saf.* **2015**, *22*, 10–19. <https://doi.org/10.1016/j.jchas.2014.11.001>.
13. Choi, K.-M.; Kim, J.H.; Park, J.H.; Kim, K.S.; Bae, G.N. Exposure Characteristics of Nanoparticles as Process By-Products for the Semiconductor Manufacturing Industry. *J. Occup. Environ. Hyg.* **2015**, *12*, D153–D160. <https://doi.org/10.1080/15459624.2015.1009983>.
14. Choi, K.-M.; An, H.-C.; Kim, K.-S. Identifying the Hazard Characteristics of Powder Byproducts Generated from Semiconductor Fabrication Processes. *J. Occup. Environ. Hyg.* **2015**, *12*, 114–122. <https://doi.org/10.1080/15459624.2014.955178>.
15. Kim, E.A.; Lee, H.E.; Ryu, H.W.; Park, S.H.; Kang, S.K. Cases Series of Malignant Lymphohematopoietic Disorder in Korean Semiconductor Industry. *Saf. Health Work* **2011**, *2*, 122–134. <https://doi.org/10.5491/SHAW.2011.2.2.122>.
16. Kim, M.-H.; Kim, H.; Paek, D. The Health Impacts of Semiconductor Production: An Epidemiologic Review. *Int. J. Occup. Environ. Health* **2014**, *20*, 95–114.
17. Jiang, W.; Lin, S.; Chang, C.H.; Ji, Z.; Sun, B.; Wang, X.; Li, R.; Pon, N.; Xia, T.; Nel, A.E. Implications of the Differential Toxicological Effects of III-V Ionic and Particulate Materials for Hazard Assessment of Semiconductor Slurries. *ACS Nano* **2015**, *9*, 12011–12025. <https://doi.org/10.1021/acsnano.5b04847>.
18. Osborne, O.J.; Lin, S.; Jiang, W.; Chow, J.; Chang, C.H.; Ji, Z.; Yu, X.; Lin, S.; Xia, T.; Nel, A.E. Differential Effect of Micron-: Versus Nanoscale III-V Particulates and Ionic Species on the Zebrafish Gut. *Environ. Sci. Nano* **2017**, *4*, 1350–1364. <https://doi.org/10.1039/c6en00675b>.
19. Qu, J.; Wang, J.; Zhang, H.; Wu, J.; Ma, X.; Wang, S.; Zang, Y.; Huang, Y.; Ma, Y.; Cao, Y.; et al. Toxicokinetics and Systematic Responses of Differently Sized Indium Tin Oxide (ITO) Particles in Mice via Oropharyngeal Aspiration Exposure. *Environ. Pollut.* **2021**, *290*, 117993. <https://doi.org/10.1016/j.envpol.2021.117993>.
20. Ham, S.; Yoon, C.; Kim, S.; Park, J.; Kwon, O.; Heo, J.; Park, D.; Choi, S.; Kim, S.; Ha, K.; et al. Arsenic Exposure during Preventive Maintenance of an Ion Implanter in a Semiconductor Manufacturing Factory. *Aerosol Air Qual. Res.* **2017**, *17*, 990–999. <https://doi.org/10.4209/aaqr.2016.07.0310>.
21. Oberdörster, G.; Oberdörster, E.; Oberdörster, J. Nanotoxicology: An Emerging Discipline Evolving from Studies of Ultrafine Particles. *Environ. Health Perspect.* **2005**, *113*, 823–839. <https://doi.org/10.1289/ehp.7339>.
22. Dankovic, D.A.; Kuempel, E.D. Current Intelligence Bulletin 63: Occupational Exposure to Titanium Dioxide. 2011, (NIOSH) 2011-160; pp. 1–140. Available online: https://stacks.cdc.gov/view/cdc/5922/cdc_5922_DS1.pdf (accessed on 9 May 2023).
23. Howard, J. Current Intelligence Bulletin 65: Occupational Exposure to Carbon Nanotubes and Nanofibers. *DHHS Public* **2013**, *2013*, 145.

24. Maher, B.A.; Ahmed, I.A.M.; Karloukovski, V.; MacLaren, D.A.; Foulds, P.G.; Allsop, D.; Mann, D.M.A.; Torres-Jardón, R.; Calderon-Garciduenas, L. Magnetite Pollution Nanoparticles in the Human Brain. *Proc. Natl. Acad. Sci. USA* **2016**, *113*, 10797–10801. <https://doi.org/10.1073/pnas.1605941113>.
25. Prüst, M.; Meijer, J.; Westerink, R.H.S. The Plastic Brain: Neurotoxicity of Micro- and Nanoplastics. *Part. Fibre Toxicol.* **2020**, *17*, 24. <https://doi.org/10.1186/s12989-020-00358-y>.
26. Singh, S. Zinc Oxide Nanoparticles Impacts: Cytotoxicity, Genotoxicity, Developmental Toxicity, and Neurotoxicity. *Toxicol. Mech. Methods* **2019**, *29*, 300–311. <https://doi.org/10.1080/15376516.2018.1553221>.
27. Cary, C.; Stapleton, P. Determinants and Mechanisms of Inorganic Nanoparticle Translocation across Mammalian Biological Barriers. *Arch. Toxicol.* **2023**, *97*, 2111–2131. <https://doi.org/10.1007/s00204-023-03528-x>.
28. Tröstl, J.; Tritscher, T.; Bischof, O.F.; Horn, H.G.; Krinke, T.; Baltensperger, U.; Gysel, M. Fast and Precise Measurement in the Sub-20nm Size Range Using a Scanning Mobility Particle Sizer. *J. Aerosol Sci.* **2015**, *87*, 75–87. <https://doi.org/10.1016/j.jaerosci.2015.04.001>.
29. Stolzenburg, M.R.; McMurry, P.H. Method to Assess Performance of Scanning Mobility Particle Sizer (SMPS) Instruments and Software. *Aerosol Sci. Technol.* **2018**, *52*, 609–613. <https://doi.org/10.1080/02786826.2018.1455962>.
30. CDC-NIOSH. Elements by ICP (Nitric/Perchloric Acid Ashing). *NIOSH Man. Anal. Methods Method* **2003**, *7300*, 2003–154.
31. CDC-NIOSH. Asbestos by TEM. *NIOSH Man. Anal. Methods Method* **1994**, *7402*, 94–113.
32. Majestic, B.J.; Anbar, A.D.; Herckes, P. Elemental and Iron Isotopic Composition of Aerosols Collected in a Parking Structure. *Sci. Total Environ.* **2009**, *407*, 5104–5109. <https://doi.org/10.1016/j.scitotenv.2009.05.053>.
33. Upadhyay, N.; Majestic, B.J.; Prapaipong, P.; Herckes, P. Evaluation of Polyurethane Foam, Polypropylene, Quartz Fiber, and Cellulose Substrates for Multi-Element Analysis of Atmospheric Particulate Matter by ICP-MS. *Anal. Bioanal. Chem.* **2009**, *394*, 255–266. <https://doi.org/10.1007/s00216-009-2671-6>.
34. Kulmala, M.; Vehkamäki, H.; Petäjä, T.; Dal Maso, M.; Lauri, A.; Kerminen, V.M.; Birmili, W.; McMurry, P.H. Formation and Growth Rates of Ultrafine Atmospheric Particles: A Review of Observations. *J. Aerosol Sci.* **2004**, *35*, 143–176. <https://doi.org/10.1016/j.jaerosci.2003.10.003>.
35. Occupational Chemical Database Home Page. Available online: <https://www.osha.gov/chemicaldata/> (accessed on 9 May 2023).

Disclaimer/Publisher’s Note: The statements, opinions and data contained in all publications are solely those of the individual author(s) and contributor(s) and not of MDPI and/or the editor(s). MDPI and/or the editor(s) disclaim responsibility for any injury to people or property resulting from any ideas, methods, instructions or products referred to in the content.